

PRACTICAL APPLICATION OF COHERENT LIGHT SCATTERING ON NANOFUIDS DYNAMICS SIMULATION

D. Chicea^{1*}, E. Culea², L. David³

¹University Lucian Blaga of Sibiu, Dr. Ion Ratiu Str. 7-9, Sibiu, 550012, Romania

²Technical University Cluj Napoca

³Babeş-Bolyai University, Cluj Napoca

Abstract:

Nanofluids are suspensions of nano to micrometer sized particles in liquids. The nanoparticles act as scattering centers when light passes through the medium. In a suspension the SCs have a complex movement of both sedimentation and the Brownian motion. As a result of the SCs permanent position changes the speckle image is not static but presents time fluctuations. A computer code to simulate the dynamics of the coherent light scattering on nanofluids was written, tested and used to calculate the far field intensity variation for nanofluids having different particle size. The results are discussed and an experimental method for fast nanoparticle size assessing is suggested.

Keywords: *nanoparticles, suspensions, computer simulation*

1. Introduction

The nanofluid notion is a relatively new notion and was first mentioned by Choi in 1995 [1] as he noticed that a small amount of nanoparticles, added in a fluid, considerably enhanced the heat transfer properties [2].

The nanoparticles have a continuous, irregular motion in nanofluids, which is the effect of several factors such as gravity, Brownian force, Archimede's force and friction force between fluid and the particles. The irregular nanoparticle motion in the fluid is the cause of the remarkable enhancement of heat transfer properties of the nanofluids [3-6]. The irregular motion directly depends of the particle dimension, therefore particle velocity techniques will furnish information on the nanoparticle size.

Measuring the nanoparticle velocity resembles much measuring the velocity distribution of flow field by seeding fluids with small particles, like the particle image velocimetry, laser Doppler velocimetry and laser speckle

* Corresponding author: dan.chicea@ulbsibiu.ro

velocimetry techniques, therefore the computer experiment presented in this work considers a speckle analysis technique [7], [8].

The seeding particles must scatter enough light to produce a good signal-to-noise ratio in order to be proper for laser particle velocimetry, therefore the diameter of the seeding particle is typically in the micrometer range. The nanoparticles though have a much smaller diameter, around 10 nanometers [9] and the intensity of the scattered light is much smaller. Results of experimental work done on coherent light scattering by nanoparticles was reported in [10] and [11] but they refer to processing the static far field images, not the light scattering dynamics. In this work a program to simulate the dynamics of the light scattering by nanoparticles is described and the results of the simulation for nanoparticles with different diameters, concentration and temperature are presented.

2. The code

When a medium having scattering centers randomly distributed is the target for a coherent light beam, an un-uniformly illuminated image is obtained, currently named speckled image, as a result of the interference of the wavelets scattered by the scattering centers (SC hereafter). The image changes in time as a consequence of the scattering centers complex movement of sedimentation and Brownian motion. This produces fluctuations of the image intensity in each location of the interference field. These fluctuations give the aspect of “boiling speckles” [7] [8]. In this work the objective speckle [7], respectively far field speckle [8] is considered.

2.1 Algorithm details

The program considers coherent light having the wavelength (which is one of the input parameters) of 632 nm to be incident on a cuvette containing the suspension. The active area of the glass cuvette (beam transversal area and light pass) are adjusted as input parameters, as well. The far field interference pattern was calculated at a distance D apart from the simulated cuvette. The cuvette is considered to be located within the coherence length of the light source. The schematic of the computer simulation setup is presented in Figure 1. As it is pointed out in [11] and other papers dealing with Rayleigh light scattering, when a nanoparticle is illuminated by a monochromatic polarized light, the polarization of its Rayleigh scattering wavelets at different points in space are different. A polarizer placed in the beam before the cuvette ensures that incident coherent light is polarized. The second polarizer, placed before the screen, having the polarization direction parallel with the polarization direction of the first one, ensures that the wavelets will actually interfere and that the screen is not illuminated with differently polarized light that will blur the image and therefore reduce the coherent effects.

Other input parameters for the simulation are: the total number of SCs, the

wavelength, an arbitrary intensity of the electric field E_0 , the cuvette – screen distance D , the x and y coordinates of the corner of the calculation area, the “pixel” dimension, the number of pixels on X and Y directions, the total number of time steps (frames) to be calculated, the number of time steps per second (frames per second), the volume and light scattering cross section of an individual SC, the light scattering anisotropy parameter g , dynamic viscosity coefficient of the fluid and finally the temperature, which is required for the Brownian motion simulation.

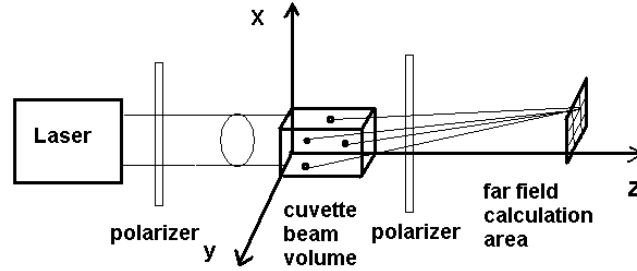


Fig. 1 – The schematic of the computer simulation

First the scattering centers positions were generated in the active area of the cuvette using random numbers with uniform distribution. The pixel size on the simulated interference field was chosen to be the same as the pixel size of the CMOS matrix of a web camera that had the optical system removed, therefore the CMOS was used to record the far field interference movie of the real system that was later on simulated, in order to compare the real far field images with the calculated images.

Unlike in [11], the single act light scattering anisotropy on a SC was modeled using the one parameter, single scattering Henyey Greenstein phase function [12], [13] (1).

$$f(\mu) = \frac{1}{2} \frac{1 - g^2}{(1 - 2\mu g + g^2)^{\frac{3}{2}}} \quad (1)$$

where $\mu = \cos(\theta)$. The anisotropy parameter, g , is currently defined as the mean cosine of the polar scattering angle θ , $g = \langle \cos(\theta) \rangle$. Consequently, for light scattering strongly peaked in the forward direction, the anisotropy parameter g is close to 1 while for isotropic scattering it is zero.

The complex amplitudes of the electric field intensity scattered by each SC were added on each pixel the assumed conversion matrix area was divided into. The electric field intensity of the interference field of a specific pixel on the screen is proportional to the integral of the f function in (1) over the cosine of the polar angle interval, $[\mu_1, \mu_2]$ and with $\Delta\phi$, the azimuthal angle interval covered by the pixel and is described by equation (2):

$$E(d, \theta, \varphi) = \frac{E_0 S_0}{d} \cdot \frac{1 - g^2}{2g} \cdot \left[\left(\frac{1}{\sqrt{1 + g^2 - 2\mu_2 g}} \right) - \left(\frac{1}{\sqrt{1 + g^2 - 2\mu_1 g}} \right) \right] \cdot \Delta\varphi \quad (2)$$

In (2) d is the actual SC – pixel distance, E_0 a constant as described above and S_0 the SC area (cross section).

At each simulation time step the SCs were moved in the active area considering both the uniform sedimentation and the Brownian motion and details on modeling these types of motions are described in the next subsection.

2.2 Sedimentation motion modeling

The sedimentation motion of the SC carries on with a constant velocity, which is the consequence of the null resultant of three forces: gravity, Archimede's force and the viscous force in laminar flow regime (Stokes). Considering the SC with a spherical shape, the velocity is given by equation (3):

$$v_s = \frac{2r^2 g}{9\eta} \cdot (\rho - \rho_0) \quad (3)$$

where r is the radius of the sphere, ρ is the density of the scattering center, ρ_0 is the density of the fluid, η is the dynamic viscosity coefficient of the fluid. The fluid was considered to be water and the variation of the water density and dynamic viscosity with temperature was calculated with a polynomial of degree 4. The coefficients were found by performing a polynomial fit on the experimental data in [14]. The sedimentation motion was modeled for each SC individually by changing the position with a distance equal with the v_s times the time step. The time step for modeling the sedimentation motion is the inverse of the framerate, which is one of the input parameters. The framerate is actually the framerate used in calculating a movie or the sampling rate, which is the time interval between two consecutive readings of the data acquisition system used in recording a time series during a laboratory experiment.

2.3 Brownian motion modelling

The Brownian motion was modeled differently, though individually for each SC. The Maxwell – Boltzman velocity distribution is actually the product of the three velocity distribution function for one dimension:

$$f_v(v_i) = \sqrt{\frac{m}{2\pi kT}} \cdot \exp\left(-\frac{mv_i^2}{2kT}\right) \quad (4)$$

In (4) k is Boltzman's constant, T is the absolute temperature and m is the mass of the particle in thermal equilibrium with the environment and i can be either x , y or z .

At each simulation time step the velocity values for v_x , v_y and v_z of each SC were therefore generated using random numbers with a normal distribution having the variance kT/m .

It should be noted that in order to have a realistic Brownian motion modeling, the time step for the Brownian motion must be different of the time step used to model the sedimentation and details on assessing it are presented in detail in [15].

2.4 Other details

Beyond the constant phase change of the wavelets emitted by each SC, there does exist another major source of the light intensity fluctuations in each location of the interference field, namely the variation of the number of SCs in the beam area. As both sedimentation motion (less significant for nanoparticles but significant for micron size particles, [15]) and Brownian motion continue, some SCs are relocated outside the beam area and other particles get inside the beam area.

In order to consider the sedimentation motion, at the beginning of the computer experiment the SCs positions are generated in a volume that has the height:

$$h = h_0 + v_s \cdot t_{\text{exp}} \quad (5)$$

where v_s is the sedimentation motion velocity, given by (3) and t_{exp} is the time span of the experiment.

As the Brownian motion is the major cause of the SCs number in the beam area variation, at the beginning of the experiment both the initial volume the SC positions were generated into and the total SC number were increased accordingly, on X, Y and Z direction, in order to maintain the particle concentration to the desired value. Each border of the beam volume in the cuvette was pushed towards outside with the square root of the quantity in (6), where t_{exp} is the time span of the experiment.

$$\begin{aligned} \langle x^2(t) \rangle &= \langle y^2(t) \rangle = \langle z^2(t) \rangle = \\ &= \int_{-\infty}^{+\infty} \int_{-\infty}^{+\infty} \int_{-\infty}^{+\infty} x^2 \cdot P(\vec{r}, t) \cdot dx dy dz = 2Dt_{\text{exp}} \end{aligned} \quad (6)$$

For a realistic modeling only the contribution of the SCs located in the beam area at that moment must be added to compute the far field intensity. Consequently after each sedimentation time step the SCs were individually moved accordingly to the sedimentation and the Brownian motion (whith the number of Brownian motion time steps required), their new positions were checked to be inside the beam area. Only the complex amplitudes of the wavelets scattered by the SCs located inside the cuvette beam volume were added in each location of the far field.

The program execution can be customized by adjusting the control parameters. It can be used to compute either an image of the far field, or a movie, with the desired framerate and resolution, in a certain location of the far field, or the

time series of the light intensity recorded by a detector with a certain dimension and location in the far field. Some results of the computer simulations are presented in the next section.

3. Computer simulation results

First the control parameters were adjusted to calculate a far field movie. A frame from the computed movie having 10 nm diameter nanoparticles as target is presented in Fig. 2.

The movie has a boiling speckles aspect, exactly as a movie recorded during a laboratory light scattering experiment on diluted magnetic fluid.

Once the code was tested, it was run to calculate images rather than movies.

The program was run first for targets with particles having a constant diameter, but with different SC numbers, hence different volume ratios, in the range $0 - 6 \cdot 10^{-13}$ and produced computed bitmaps. The average intensity was calculated for each target and the variation of the average intensity $\langle I \rangle$ with the nanoparticles volume ratio is presented in Fig. 3.

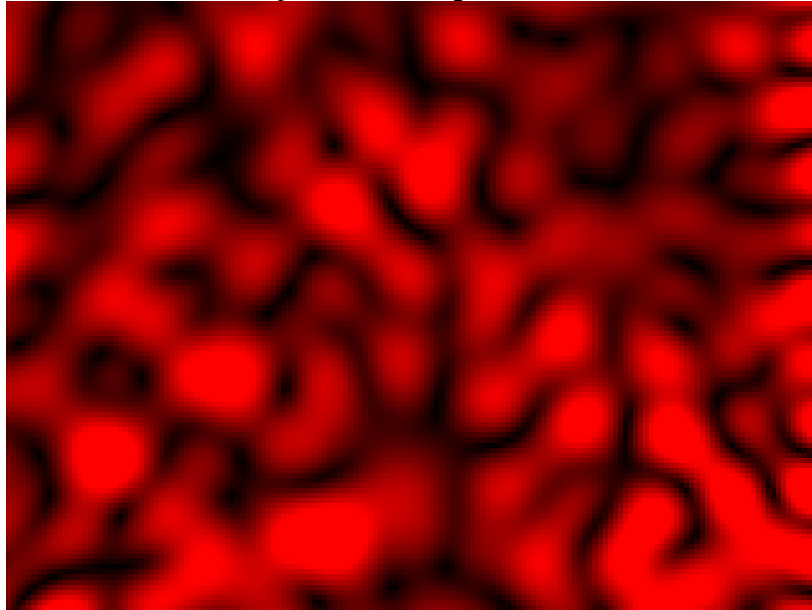


Fig. 2 - A computed far field image having 7 nm diameter nanoparticles as target.

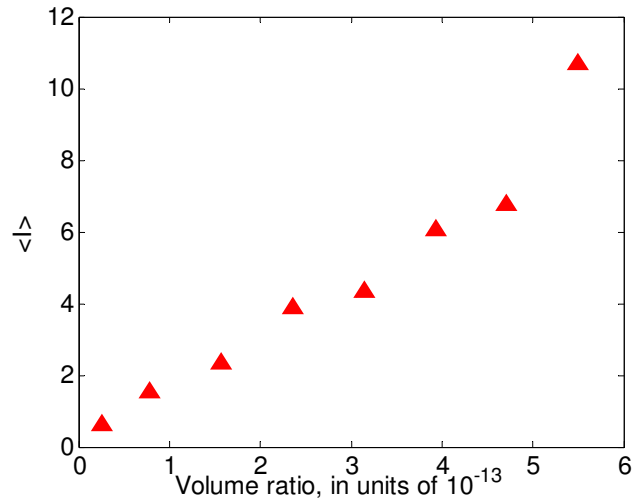


Fig. 3 - The average intensity variation with the nanoparticles volume ratio

Examining Fig. 3 we notice an increase of the average scattered light intensity, $\langle I \rangle$ with the nanoparticles volume ratio, at constant nanoparticle diameter. This variation, if confirmed by experiments, can be used to measure the nanoparticle concentration in the very small values range, more precisely in the parts per billion range.

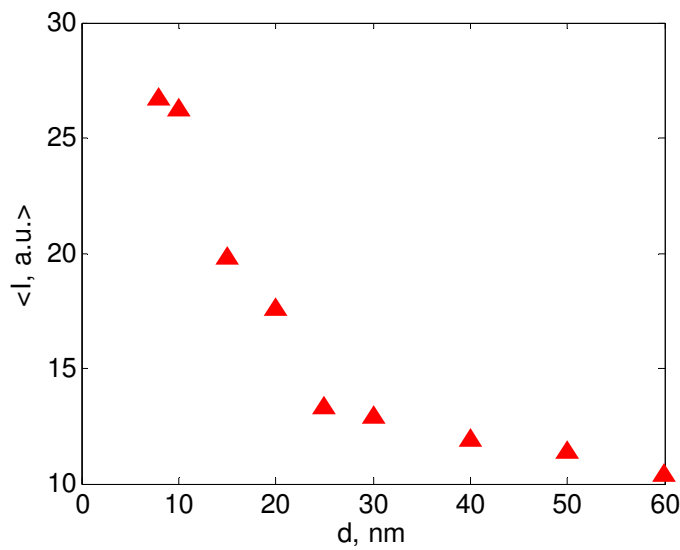


Fig. 4 - The average intensity variation with the particle diameter, for samples having a volume ratio equal to $5.0 \cdot 10^{-13}$

During a laboratory experiment the SC number can not be easily determined but the volume ratio can be experimentally adjusted precisely for a sample. A computer experiment considered different samples having the same volume ratio but different particle diameters, hence different SC physical parameters and number. For each type of suspension a bitmap image was calculated, having a volume ration of 5.0·10⁻¹³ and particle diameters from 7 to 60 nm. The average intensity variation with the particle diameter, for samples having a constant volume ratio, is presented in Fig. 4

Examining Fig. 4 we notice a monotone decrease of the average intensity with increasing the particle size, especially in the small nanoparticle size range, which is of interest for biomedical applications [16]. This trend, if confirmed by laboratory experiments, suggests a fast procedure for assessing the average nanoparticle size right after synthesis. Several calibration experiments must be done, with samples having different particle diameter and the same volume ratio. For each experiment a bitmap is recorded and the average intensity is calculated. A calibration curve like Fig. 4 is drawn. For a new sample the procedure is repeated and the average intensity is calculated. Using the calibration curve the average nanoparticle size can be assessed.

Another way of processing the computed far field bitmaps consists of calculating the contrast and the average speckle size. The average contrast and the average speckle size variation with the particle size were calculated with the program described in [17]. Their variation is not as strong as the average intensity variation, therefore they are not presented here.

Running the program with another value of the control parameter, a time series representing the far field intensity fluctuations was calculated. The cuvette-detector distance was 0.8 m, the detector was 0.005 m apart from the beam direction, therefore coherent light scattered at 0o21'29" was calculated. The detector was assumed to cover a solid angle of 1.1·10⁻⁵ sr. The autocorrelation function of each of the generated time series was calculated with (7) [18]:

$$A(\tau) = \frac{\langle E(\vec{r}, t) * E(\vec{r}, t + \tau) \rangle}{\langle E(\vec{r}, t) * E(\vec{r}, t) \rangle} \quad (7)$$

where the angle brackets denote averages over time t, r represents the position of the detector, and τ is the correlation time. The normalized autocorrelation function decreases from 1 and we can define the autocorrelation time τ as the time when the autocorrelation function decreases to 1/e.

The program was run for particles with a diameter in the range 4 – 37 nm and produced time series for each target. The autocorrelation time was calculated for each target. The sampling rate of the assumed data acquisition system was 10000 per second. It is worth mentioning that the computer time required to produce a time series is very big, as the motion of each SC is individually calculated and tracked, growing linearly both with the length of the time series and with the SC

number.

The variation of the autocorrelation time with the SC diameter, for a constant number of nanoparticles, is presented in Fig. 5. Examining Fig. 5 we notice that the calculated data has a relatively big spread. Nevertheless, an increase of the autocorrelation time with the size of the nanoparticles is obvious.

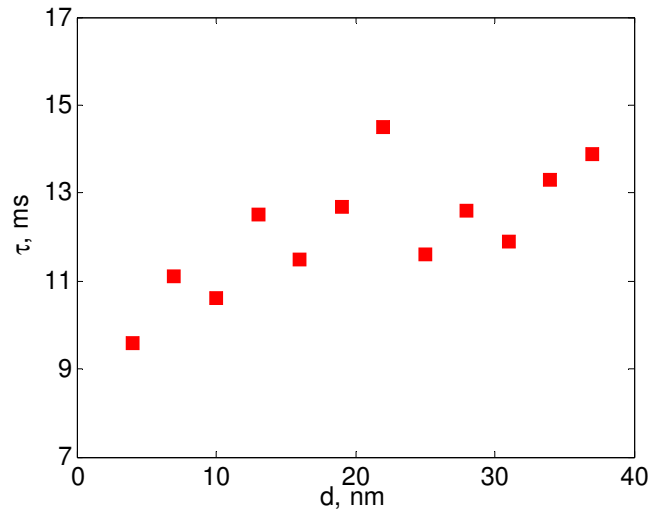


Fig. 5 – The autocorrelation time variation with the SC diameter, at constant SC number.

Another type of experiment of coherent light scattering experiment was conducted in a slightly different manner, maintaining the SC number constant and changing the temperature. The Maxwell – Boltzmann distribution shifts toward bigger velocities when the absolute temperature T increases. A time series was generated for each temperature and the autocorrelation time was calculated for each series, as described before. Fig. 6 presents the variation of the autocorrelation time with the absolute temperature, at constant SC number. Examining Fig. 6 we notice a fast decrease of the autocorrelation time with the temperature increase.

4. Conclusion

A simple algorithm for assessing the time step for modeling the Brownian motion is described and used in simulating the static and the dynamic coherent light scattering on nanofluids. The results of the computer simulation presented above were compared with the images and the movies recorded during a coherent light scattering experiment on nanofluids. The computer simulation describes accurately both the far field interference aspect and the light scattering dynamics.

The time series computed during the computer experiment were analyzed and the

autocorrelation function was calculated and compared with the autocorrelation function of a time series recorded during a laboratory experiment performed on the real system with the same parameters. An interesting result that emerged is that the autocorrelation time increased when the nanoparticle velocities decrease, regardless the cause of the decrease, although the nanoparticle velocities are randomly oriented.

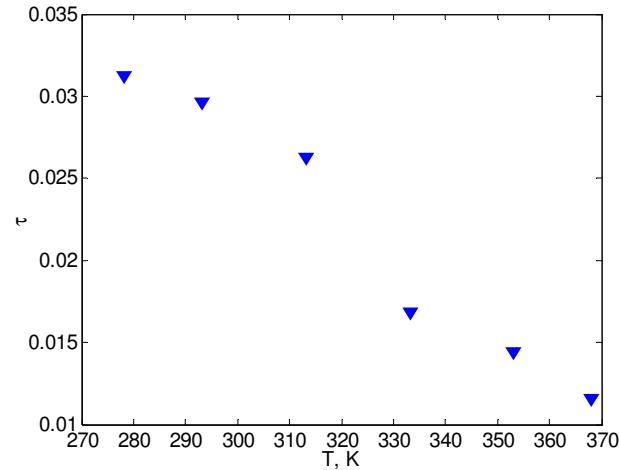


Fig. 6 - the variation of the autocorrelation time with the absolute temperature

The nanoparticle size is one of the most important parameters that dictate the properties of a nanofluid or magnetic fluid. The computer simulation results presented in this work suggest two simple and low cost procedures for assessing the nanoparticle size. The first one requires a measurement of the light scattering intensity at constant angle and, most important, at constant volume ratio, which can be adjusted accurately using common laboratory equipment. A calibration curve, light intensity versus nanoparticle diameter, at constant volume ratio, like Fig. 4, is drawn first using nanoparticles with a precisely known diameter, measured using TEM or other conventional method. The curve can be used later on in measuring the nanoparticle diameter for a new prepared sample.

Another interesting result that was found running the computer simulation is that the autocorrelation time of a calculated time series decreases with the increase of the nanoparticle size, at constant nanoparticle number, and this result suggested the second method proposed by this article for indirect particle sizing. For each nanofluid sample with precisely known nanoparticle diameter a time series must be recorded using a detector and a data acquisition system, in the same detection geometry. The autocorrelation time is calculated for each recorded time series. A calibration curve can be interpolated and used further on to assess the mean diameter of a nanofluid with unknown particles in suspension. If confirmed by accurate experimental results, the methods proposed in this paper are much faster

and have a considerable lower cost than using an electron microscope or other conventional methods.

The methods appear to be less precise, as calculated data has a big spread. Further improvement by using a faster computer and longer computation time series is scheduled, to verify the hypotheses stated in this article.

References

- [1] U. S. Choi, "Enhancing thermal conductivity of fluids with nanoparticles," ASME Fed. 231, 99-103 (1995).
- [2] P. Vadasz, "Heat conduction in nanofluid suspensions," J. Heat Transfer. 128, 465-477 (2006).
- [3] S. P. Jang and S. U. S. Choi, "Role of Brownian motion in the enhanced thermal conductivity of nanofluids," Appl. Phys. Lett. 84, 4316-4318 (2004).
- [4] W. Evans, J. Fish and P. Keblinski, "Role of Brownian motion hydrodynamics on nanofluid thermal conductivity," Appl. Phys. Lett. 88, 093116 (2006).
- [5] Y. M. Xuan and W. Roetzel, "Conceptions for heat transfer correlation of nanofluids," Int. J. Heat Mass Transfer. 43, 3701-3707 (2000).
- [6] R. Prasher, P. Brattacharya and P. E. Phelan, "Thermal conductivity of nanoscale colloidal solutions (nanofluids)," Phys. Rev. Lett. 94, 025901 (2005).
- [7] J.W. Goodman, "Statistical Properties of Laser Speckle Patterns," in Laser speckle and related phenomena, Vol.9 in series Topics in Applied Physics, J.C. Dainty, Ed., Springer-Verlag, Berlin, Heidelberg, New York, Tokyo, (1984).
- [8] J David Briers, *Physiol. Meas.* 22, R35–R66, (2001).
- [9] W.X. Fang, Z.H. He, X.Q. Xu, Z.Q. Mao and H. Shen, "Magnetic-field-induced chain-like assembly structures of Fe₃O₄ nanoparticles", *European Physics Letters* 77 68004, (2007).
- [10] D. Chicea, M. Răuciu, "On magnetic fluid synthesis and light scattering anisotropy parameter," *JOAM* 9, nr.9,2738, (2007).
- [11] Ming Qian, Jun Liu, Ming-Sheng Yan, Zhong-Hua Shen, Jian Lu and Xiao-Wu Ni, "Investigation on utilizing laser speckle velocimetry to measure the velocities of nanoparticles in nanofluids," *Optics Express* 14, No. 17, 7559, (2006).
- [12] I. C. Kim and S. Torquato, "[Effective conductivity of suspensions of hard spheres by Brownian motion simulation](#)", *J. Appl. Phys.* 69, 2280, (1991).
- [13] M. Hammer, D. Schweitzer, B. Michel, E. Thamm, A. Kolb, "Single scatter by red blood cells", *Applied Optics* 37, 7410-7419, (1998).
- [14] "Physical characteristics of water", http://www.thermexcel.com/english/tables/eau_atm.htm
- [15] D. Chicea, "Coherent light scattering on nanofluids - computer simulation results", submitted to *Applied Optics*, manuscript no. 88852.
- [16] Q.A. Pankhurst, J. Connolly, S.K. Jones, J. Dobson, "Applications of magnetic

nanoparticles in biomedicine”, J. Phys. D, 36, R167 (2003).

[17] D. Chicea, “Speckle size, intensity and contrast measurement application in micron-size particle concentration assessment”, Accepted to be published in European Physical Journal – Applied Physics.

[18] R. Bracewell, The Fourier Transform and Its Applications, 3rd ed. New York: McGraw-Hill, pp. 40-45, (1999).